

TECHNICAL ARTICLE

Techno-Economic Analysis of Standalone Solar Photovoltaic-Wind-Biogas Hybrid Renewable Energy System for Community Energy Requirement

Vijay Mudgal*, K. S. Reddy* and T. K. Mallick†

Integrated renewable energy system (IRES) is integration of different energy sources to provide uninterrupted and viable solution for electrification especially for areas not connected to main grid due to difficult terrain and economic reasons. IRES has many advantages like non-depleting, non-polluting nature, better load matching and better renewable energy utilization. In the present study, mathematical modelling, size optimization and techno-economic analysis of standalone IRES have been carried out. Hybrid system is modelled to have maximum contribution from wind and solar energy with minimum net present cost (NPC) of system to meet electric load demand of CRC building, IIT Madras, India (13.01°N and 80.24°E). The results show that most feasible system configuration consists of 12 kW Photovoltaics, 3 kW wind turbine and 15 kW biogas generator with NPC and cost of energy equal to \$ 117,098 and \$ 0.09/kWh respectively. The IRES generates 71,826 kWh of energy to meet AC load of 64,396 kWh per year. The capacity factor and percentage contribution of PV, wind turbine and biogas generator are 17.8%, 6.57%, 39.1% and 26%, 2.4%, 71.6% respectively. The paper also presents sensitivity analysis of hybrid system with variation in capital cost of different components.

Keywords: Renewable energy; Hybrid system; Net present cost; Cost of energy; Optimization

1. Introduction

Uninterruptible and viable power supply to every household is one of the main challenge Indian government has taken, especially in rural and remote places which due to difficult terrain or due to economic reasons not connected to the main power grid. In such locations, renewable energy sources like Photovoltaics (PV) and wind energy are gaining attention due to easy installation, higher energy utilization rate, lower power transmission loss and lower operational cost. However, unpredictable and inconsistent nature are major drawback of some of the renewable sources to provide viable power energy. To counter this different renewable and non-renewable sources can be integrated together for increased system efficiency, greater balance of energy and viable power supply (Chauhan and Saini, 2014). However, selection of components of hybrid energy system and size optimization is very important to have reliable and cost effective system. The load demand and power generation with storage need to be optimally match, so that maximum utilization of

energy sources and minimum investment can be assured. Various energy sources such as solar, wind, hydro, biomass and biogas etc. which are cost effective can be integrated together to meet viable electric load demand (Al-falahi et al., 2017). There are various advantages of IRES (i) better utilization of renewable energy (ii) better load matching (iii) better controllability (iv) less operational and maintenance cost (v) lesser environmental emission (Chong et al., 2016; Tezer et al., 2017).

Effective integration of hybrid energy sources has been gaining attention in the scientific community since past few decades to solve the technical and economic barriers for using renewable and distributed systems (Allison, 2017; Cano et al., 2017; Goel and Sharma, 2017; Kabalci, 2013; Perez-Navarro et al., 2016; Reddy et al., 2018, 2017; Yin et al., 2017). The study by Taele et al. (Taele et al., 2012) shows that installation of small scale solar PV systems at communities in Lesotho prevented frequent breakdowns, avoided large fuel storage and reduced power losses. Patil et al. (Patil et al., 2010) compared off-grid electrification of seven villages of Uttarakhand, India by integrating four different renewable energy sources to meet electrical and cooking needs. Baghadi et al. (Baghdadi et al., 2015) investigated the performance of hybrid PV-wind diesel battery system in Adrar climate of southern Algeria. The optimized system was able to meet 70% of energy demand by renewable PV-wind system and thereby reduced fossil fuel

* Heat Transfer and Thermal Power Laboratory, Department of Mechanical Engineering, Indian Institute of Technology Madras, Chennai, IN

† Environment and Sustainability Institute, University of Exeter, Penryn Campus, Penryn, Cornwall, UK

Corresponding author: K. S. Reddy (ksreddy@iitm.ac.in)

consumption. Singh et al. (Singh et al., 2017) examined technical and economic feasibility of hybrid hydrogen fuel cell and PV system to meet the energy demand of academic building at Bhopal, India. The analysis shows 3 kW hydrogen fuel cell with 5 kW of PV as most feasible system with minimum NPC and zero percentage energy shortage to meet load demand. Lau et al. (Lau et al., 2010) showed that integration of PV and diesel sources with battery can expressively reduce dependence on solely available diesel resource. Yilmaz and Selim (Yilmaz and Selim, 2013) reviewed different design techniques of biomass to energy conversion and integration of different renewable sources with biomass. The study shows that with appropriate integration of renewable energy resources and technologies, load demand can be met efficiently. Rahman et al. (Rahman et al., 2014) investigated technical and economic optimization of hybrid biomass and photovoltaic system to meet both thermal (cooking) and electric loads, replacing conventional facilities.

Ozden and Tari (Ozden and Tari, 2016) studied exergy and energy analysis of hybrid solar-hydrogen system in Ankara, Turkey. The result shows that overall hybrid system efficiency and hydrogen cycle efficiency are 6.21% and 4.06% respectively. The authors also suggested that PV-hydrogen hybrid system is better than PV-battery system. Using inspired coevolutionary algorithm Shi et al. (Shi et al., 2015) designed hybrid energy system with PV, wind turbines, batteries and diesel generator. The optimization of the system includes minimization of annualized cost of the system, loss of power supply probability and fuel usage. A multi-objective receding horizon optimization is proposed by Forough and Roshandel (Behzadi Forough and Roshandel, 2017) to determine optimal scheduling of hybrid energy system. Diesel fuel cost and battery wear cost were considered as two objective functions. Castellanos et al. (Castellanos et al., 2015) studied various combination of PV, anaerobic digester and combined heat and power unit using micro-grid modelling simulations to power a small village in West Bengal, India. The result shows that IRES containing PV, anaerobic digester, and a micro turbine has lower capital and electricity cost over the life of the project. The design and evaluation of PV-hybrid systems by M. Muselli et al. (Muselli et al., 1999) and M.R. Borges Neto et al. (Borges Neto et al., 2010) analysed the optimal contribution of system components to serve the demand. Giatrakos et al. (Giatrakos et al., 2009) presented sustainable planning of renewable based energy system by replacing existing diesel generator with hybrid PV-Wind and hydrogen system for Karpathas island of Dodecanese, Greece.

From the literature study, it has been observed that considerable work has been done on optimization of integrated system considering different configuration and optimization technique. However, most of the study did not optimize the system, considering seasonal variation in energy load demand. This is important for accurate designing of hybrid system to have maximum resource utilization with minimum system cost to meet load demand all time. Present study focus on size optimization and economic analysis of hybrid integrated renewable energy

system with seasonal load demand. Mathematical modeling, feasibility study and control strategy of all the system component has been done. Also, sensitivity analysis of hybrid system with variation in system component cost has been carried out. The optimization of integrated system has been carried out using HOMER software.

The paper is organized as follows, Section 2 describes the proposed hybrid integrated renewable energy system. Section 3 explains specification and mathematical modeling of components of proposed IRES system and seasonal electric load demand. Section 4 explains methodology, constraints and control strategy implemented in present system. Section 5 discuss size, economic and energy analysis of optimized IRES configuration and section 6 discusses sensitivity analysis of system with variation in cost of system components.

2. Description of proposed IRES

The integrated energy system must be feasible and viable, i.e. at each time step some or the other energy system i.e. primary generation, backup system or storage system must be available to meet electric load demand. To achieve this, there are many possible configurations in which system components can be designed and integrated. Probabilistic approach of simulations of system components has been carried out for sizing based on wind speed, solar radiation, biogas specification, electric load demand and certain technical and physical parameter. The schematic of proposed IRES is shown in **Figure 1**. Different component of hybrid energy system includes wind turbine, solar PV, solar charge controller, inverter, battery, control panel, and biogas generator. In the present study, wind speed, solar radiation, ambient temperature, PV temperature, wind speed, fuel property of biogas and load reading are measured by various equipment and weather monitoring system available in the solar energy research laboratory at IIT Madras, India.

For validation, modelling has been carried out similar to done by Baghdadi et al. (Baghdadi et al., 2015) using HOMER software. The simulation and calculation shows similar results to those of Baghdadi et al.

3. Specification and Mathematical modeling of IRES components

3.1. Wind energy system

The power output of the wind turbine depends upon wind speed at the location and turbine specification and is calculated by Eq. (1) (Chedid et al., 1998).

$$\begin{aligned}
 P_w(t) &= 0 & V(t) < V_{ci} \\
 P_w(t) &= \frac{P_r}{(V_r^3 - V_{ci}^3)} V^3(t) - \frac{V_{ci}^3}{(V_r^3 - V_{ci}^3)} P_r & V_{ci} \leq V(t) < V_r \\
 P_w(t) &= P_r & V_r \leq V(t) < V_{co} \\
 P_w(t) &= 0 & V(t) \geq V_{co}
 \end{aligned} \quad (1)$$

Where $V(t)$ is speed of wind at time t , P_r is wind turbine rated power and V_{ci} , V_r and V_{co} are respectively wind turbine cut in, rated and cut out speed (Tito et al., 2016).

By knowing wind profile at reference height, wind speed at any other height can be calculated by Eq. (2).

$$V_h = V_{ref} \left(\frac{H}{H_r} \right)^\alpha \tag{2}$$

Where V_h is wind speed at height H , V_{ref} is wind speed at reference height H_r , and α is wind speed power law coefficient. The overall effective electrical power output of wind turbine (P_{weff}) can be expressed as Eq. (3).

$$P_{weff} = P_w A_w \eta_w \eta_{inv} \tag{3}$$

Where A_w is wind turbine swept area, η_w is wind turbine efficiency and η_{inv} is inverter's efficiency. The wind speed for the complete year at height of 10 m above ground at

IIT Madras, India is shown in **Figure 2**. The specification of wind turbine (Luminous Whisper 500) used for present study is summarized in **Table 1**.

3.2. Solar photovoltaic system

The basic element of solar PV module is a solar cell that converts incident solar radiation directly into electrical energy (DC current) (Derrouazin et al., 2017; Khanna et al., 2017). The power output of PV array depends upon PV module specification and is calculated by Eq. (4) (Koutroulis et al., 2006).

$$P_{pv} = N_s N_p V_{oc} I_{sc} FF \tag{4}$$

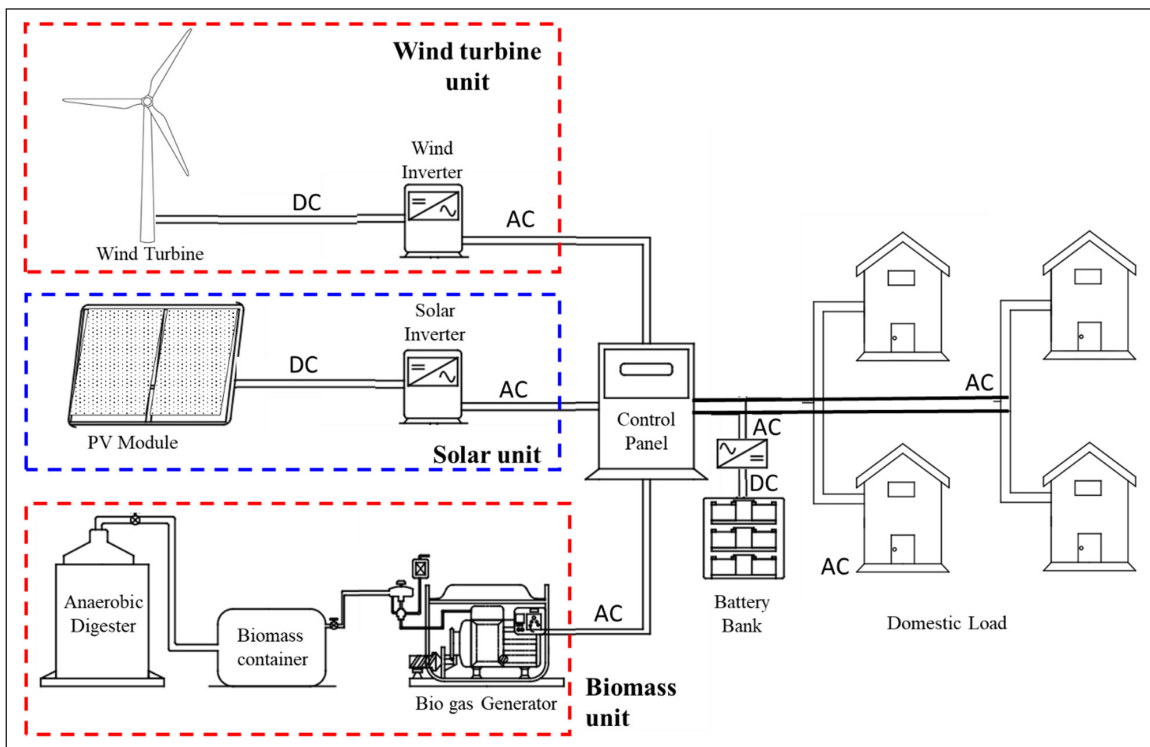


Figure 1: Schematic of integrated hybrid renewable energy system.

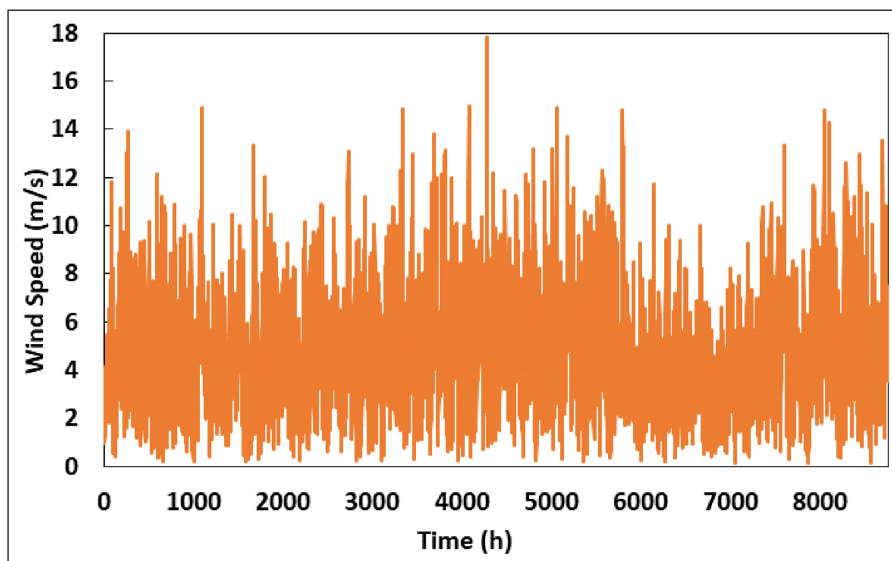


Figure 2: Wind speed profile at IIT Madras, India.

Where N_p and N_s are respectively numbers of PV modules connected in parallel and series, I_{sc} is short circuit current (A) of PV module, V_{oc} is open-circuit voltage (V) of PV module, and FF is fill factor of panel.

The overall effective power from PV array is calculated by Eq. (5).

$$P_{ar} = \eta_{mod} \eta_{inv} P_{pv} \quad (5)$$

Where η_{mod} is PV module efficiency, η_{inv} is inventor efficiency.

The effects of solar irradiance at tilted PV (I_T), solar irradiance coefficient (γ_c), average temperature of PV ($T_{pv,avg}$), temperature coefficient (β_c), efficiency of PV panel at standard test conditions (η_{stc}) and area of PV (A_{pv}) on the electrical output (E_{pv}) of the systems can be calculated by Eq. (6) (Khanna et al., 2018).

$$E_{pv} = \eta_{stc} \left\{ 1 + \beta_c (T_{pv-avg} - 25) + \gamma_c \ln \left(\frac{I_T}{1000} \right) \right\} I_T A_{pv} \quad (6)$$

The temperature of PV cell can be calculated by Eq. (7).

$$T_{pv-avg} = T_{amb} + (NOCT - 20) \frac{S_{mod}}{S_{stc}} \quad (7)$$

Table 1: Specification of wind turbine (Chauhan and Saini, 2016).

Parameter	Unit	Value
Rated Power	kW	3
Rated wind speed	ms ⁻¹	12
Cut-in wind speed	ms ⁻¹	3.1
Cut-out wind speed	ms ⁻¹	24
Rated voltage	V	240
Rotor diameter	m	4.5
Swept area	m ²	15.1

Where T_{amb} is ambient temperature, NOCT is nominal operating cell temperature (°C), S_{mod} is solar incident radiation (Wm^{-2}) on the PV module and S_{stc} is incident solar radiation at standard test condition (Wm^{-2}).

The power obtained from PV panel is directly related to the slope at which panel is installed. The maximum incident radiation on the solar panel for the given location is calculated by equation (8) (Sukhatme and Sukhatme, 1996).

$$S_{mod} = S_{inc} \sin([90 - \phi + \delta] + \gamma) \quad (8)$$

Where declination angle δ is given by,

$$\delta = 23.45 \sin[(360/365)(284 + d)] \quad (9)$$

The yearly solar radiation at CRC building, IIT Madras is calculated and compared with the Indian Meteorological Department (IMD) solar radiation database ("Indian Meteorological Department," n.d.). The average hourly month wise solar radiation profile at CRC, IIT Madras is shown in **Figure 3**. The specification of PV (Bosch solar module CSI-P 60) used for present study is summarized in **Table 2**.

3.3. Battery Bank system

The charging of battery takes place when power produced by wind turbine and PV is more than electric load demand. Battery bank is used to serve load demand when the power output of wind turbine and PV system is less than threshold value and is insufficient to meet load demand. Battery bank capacity is selected based on total power needed and autonomy period of operation in a day. The battery bank cost for complete duration of the project has three components: capital cost, operation & maintenance (O&M) cost, and replacement cost. The capital cost of battery bank depends on its size and specification, O&M cost includes maintenance cost at regular interval whereas replacement cost is cost of replacing battery after particular duration (lifetime). Thus selection of right battery bank is important during integration of system. The tabular lead acid

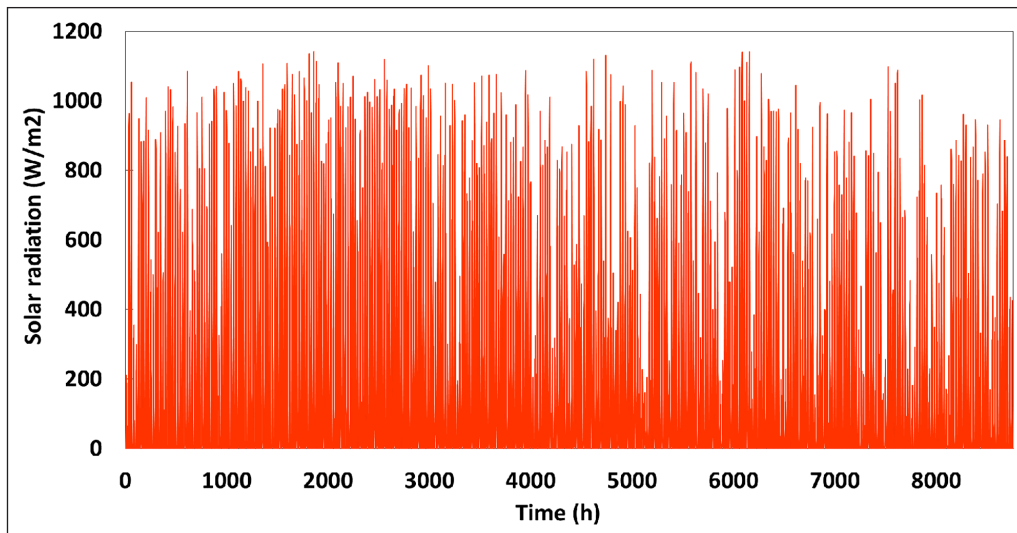


Figure 3: Solar radiation profile at CRC building, IIT Madras, India (13.01°N, 80.24°E).

batteries are largely used for solar application in India because of their low cost and robust usage. Thus, authors have considered tabular lead acid batteries for present analysis. The characterization of battery to know its charge and discharge status is determined by its state of charge (SOC). The SOC is defined as the ratio of current capacity to nominal capacity of the battery. When battery is fully charged, SOC is one and when the battery is empty, SOC is zero. The instantaneous SOC of battery can be calculated by Eq. (10) (Chiasson and Vairamohan, 2005).

$$SOC(t) = SOC(t-1) \left(1 - \frac{\sigma \Delta t}{24} \right) + \left(\frac{I_{bat}(t) \cdot \Delta t \cdot \eta_{bat}}{C_{bat}} \right) \quad (10)$$

Where SOC(t) is state of charge of battery at time t, SOC(t-1) is state of charge at (t-1) hours, σ is battery self-discharge rate, I_{bat} is battery current at time t (A), η_{bat} is battery charge efficiency and C_{bat} is capacity of battery bank.

The instantaneous battery current is given by Eq. (11) (Chiasson and Vairamohan, 2005).

$$I_{bat}(t) = \frac{P_{pv}(t) + P_w(t) - P_{load}(t)}{V_{bat}(t)} \quad (11)$$

Where $P_{pv}(t)$ and $P_w(t)$ are respectively instantaneous power generated by PV and wind turbine system, $P_{load}(t)$ is instantaneous load demand and $V_{bat}(t)$ is terminal voltage of battery bank. The capacity of the battery bank C_{bat} is given by Eq. (12) (Singh et al., 2017).

$$C_{bat} = (E_{load} AD) \eta_{inv} \eta_{bat} DOD \quad (12)$$

Where E_{load} is total energy demand, AD is daily autonomy, DOD is depth of discharge of battery, η_{inv} is inverter efficiency, and η_{bat} is battery efficiency.

Table 2: Specification of PV module (Bosch Solar Energy, n.d.).

Parameters	Value	Parameters	Value
Cell Configurations (Nos.)	60	Maximum System Voltage (DC)	1000
P_{max} (W) (Tolerance: +3%)	250	Series Fuse Rating (A)	15
V_{oc} (V) (Tolerance $\pm 3\%$)	37.00	Nominal Operating Cell Temp. ($^{\circ}C$)	44.6
I_{sc} (A) (Tolerance $\pm 3\%$)	8.55	Temp. Coefficient of P_{max} ($\%/^{\circ}C$)	-0.45
V_{max} (V) (Tolerance $\pm 3\%$)	30.95	Temp. Coefficient of V_{oc} ($\%/^{\circ}C$)	-0.36
I_{max} (A) (Tolerance $\pm 3\%$)	8.08	Temp. Coefficient of I_{sc} ($\%/^{\circ}C$)	0.043

Table 3: Specification of generator (*Specification, Test generator. Sawafuji Electric Co., Ltd, ELEMAX Generator SH7600EX: Owner's Manual, n.d.*).

Parameter	Specification
Model	ELEMAX SH5300EX Generator
Engine type	4 stroke, single cylinder, side valve, Spark Ignition engine
Ignition system	Transistorized Coil Ignition (TCI)
Rated Power	6.3 kW @ 3600 rpm
Generator AC output	5.3 kVA @ 220 V, 60 Hz
Cooling system	Forced Air Cooling

3.4. Biogas generator system

The biogas generator (Bio-Gen) is used as secondary power source for the proposed IRES system. The generator is used to meet peak load and when PV, wind turbine and battery power are insufficient to fulfill load demand. Biogas is used as fuel by biogas generator to produce electrical power. The biogas is produced by biodegradation of organic material fed into gasifier. The power output of biogas generator is given by Eq. (13) (Liu et al., 2018).

$$P_{bio} = \frac{B \cdot C_{VBG} \cdot \eta_{BG} \cdot \eta_{gas}}{3600} \quad (13)$$

Where B is amount of biomass, C_{VBG} is calorific value of biogas ($kJ \cdot kg^{-1}$), η_{BG} is efficiency of biogas generator and η_{gas} is efficiency of gasification of gasifier. The specification of generator considered for present study is listed in **Table 3** (*Specification, Test generator. Sawafuji Electric Co., Ltd, ELEMAX Generator SH7600EX: Owner's Manual, n.d.*).

3.5. Converter system

Power converter is required to maintain flow of energy from different power sources of IRES to electric load by converting electric energy from one form to another (AC to DC and vice versa) (Zahboune et al., 2016). The power generated by wind turbine, solar PV and power stored in battery bank is in DC form. Whereas, power generated by biogas generator and electric load is in AC form. Converter is a combination of both inverter (DC to AC) and rectifier (AC to DC), which operate as per the requirement of flow of energy (Kabalci, 2013).

3.6. Load demand Profile

The electric load profile is the main influencing factor for designing and optimizing of integrated hybrid energy system. So, it is very important to know how load vary from

weekdays to weekends and from season to season for accurate designing of hybrid system to have maximum utilization of resources and minimum system cost. The electric loads considered for present study are computers, fans, lights, electronic devices and machinery. The load demand of the building varies with weather condition. Chennai has three major seasons' summer, monsoon and winter. March to August is summer season, September to October is monsoon season and November to February is winter season. The seasonal average electric load profile and frequency histogram of load for CRC building, IIT Madras is shown in **Figure 4**.

4. Optimization and Operational methodology

4.1. Component sizing and optimization

The optimization of integrated hybrid system has been done by HOMER software. The software simulates all possible system configurations to find the optimum combination of hybrid system to match seasonal electric load demand (Al Garni et al., 2018). Various details like global solar radiation, ambient temperature, wind speed, specification of components, electric load demand are given as input for the simulation. The specification of system component and load demand of proposed IRES are described in section 3. The HOMER software determine various system combination in terms of economic and technical parameters. In present work optimization is done on the basis of net present cost of hybrid system.

4.1.1. Net present cost

The proposed optimisation process is based on lowest NPC of the system which is total of capital cost, O&M cost, replacement cost and salvage cost of the integrated system over the project life. The net present cost of the system calculated by HOMER is given by Eq. (14) (Dalton et al., 2008).

$$C_{NPC} = \frac{C_{ann}}{CRF(i, R_{proj})} \tag{14}$$

Where C_{ann} is annualized cost, CRF is capital recovery factor, i is annual real discount rate, R_{proj} is project lifetime (25 years).

4.1.2. Capital recovery factor

The capital recovery factor is ratio used to calculate present value of an annuity that is amount of cash flow annually over the lifetime of the project and is given by Eq. (15) (Li et al., 2013).

$$CRF(i, R_{proj}) = \frac{i(1+i)^{R_{proj}}}{(1+i)^{R_{proj}} - 1} \tag{15}$$

Where i is nominal discount rate.

4.1.3. Cost of energy

The levelized cost of energy (COE) is average cost to generate per kWh of useful electrical energy by integrated system. It is one of the important economic assessment factor considered while optimizing integrated energy system. It is the ratio of total annualized cost (C_{ann}) of system to useful energy served (E_{ser}) by the system and is calculated by Eq. (16) (Li et al., 2013).

$$COE = \frac{C_{ann}}{E_{ser}} \tag{16}$$

4.1.4. Salvage cost

Salvage cost (C_{sal}) is value of the components of integrated system at the end of the project. The salvage cost is calculated by Eq. (17) (Munuswamy et al., 2011).

$$C_{sal} = C_{rep} \frac{R_{rem}}{R_{comp}} \tag{17}$$

Where C_{rep} is component's replacement cost, R_{rem} is component's remaining life, R_{comp} is the lifetime of the project.

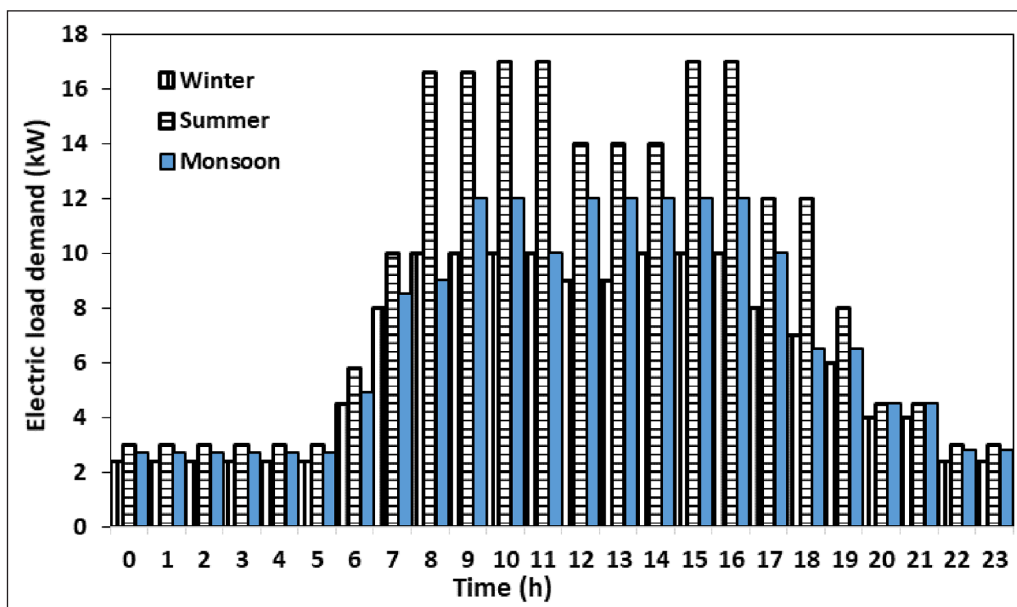


Figure 4: Seasonal load demand at CRC, IIT Madras.

The real discount rate is used to convert between one-time cost and annualized cost and is calculated by Eq. (18) (Li et al., 2013).

$$i = \frac{i' - f}{1 + f} \tag{18}$$

Where i' is nominal discount rate and f is expected inflation rate.

Present operational strategy aim at maximizing wind and solar PV energy utilization and reducing operational duration of biogas generator and thereby reducing pollutant

emission. Economic data and operation life of different components of integrated hybrid energy system are listed in **Table 4**.

4.2. Control strategy

The dispatch strategy for IRES is a control algorithm of interaction among various system components. The control operation is done on the basis of percentage of accurate load demand, wind turbine & PV power output and state of charge of battery. **Figure 5** shows flow chart of operational strategy of the system. Calculation of value these parameter is important to achieve optimum

Table 4: Economic data and operational life of components of IRES.

Component	Capital cost (in \$)	O & M cost (in \$)	Replacement cost (in \$)	Life
Wind turbine	1667/kW	50/kW/year	1667/kW	25 year
Solar PV	925/kW	25/kW/year	925/kW	25 year
Solar inverter and control panel	198/kW	8/kW/year	198/kW	10 year
Battery (200 Ah, 12 V)	153/batt	7/batt/year	125/batt	5 year
Biogas-generator	470/kW	0.01/kWh	380/kW	20,000 h

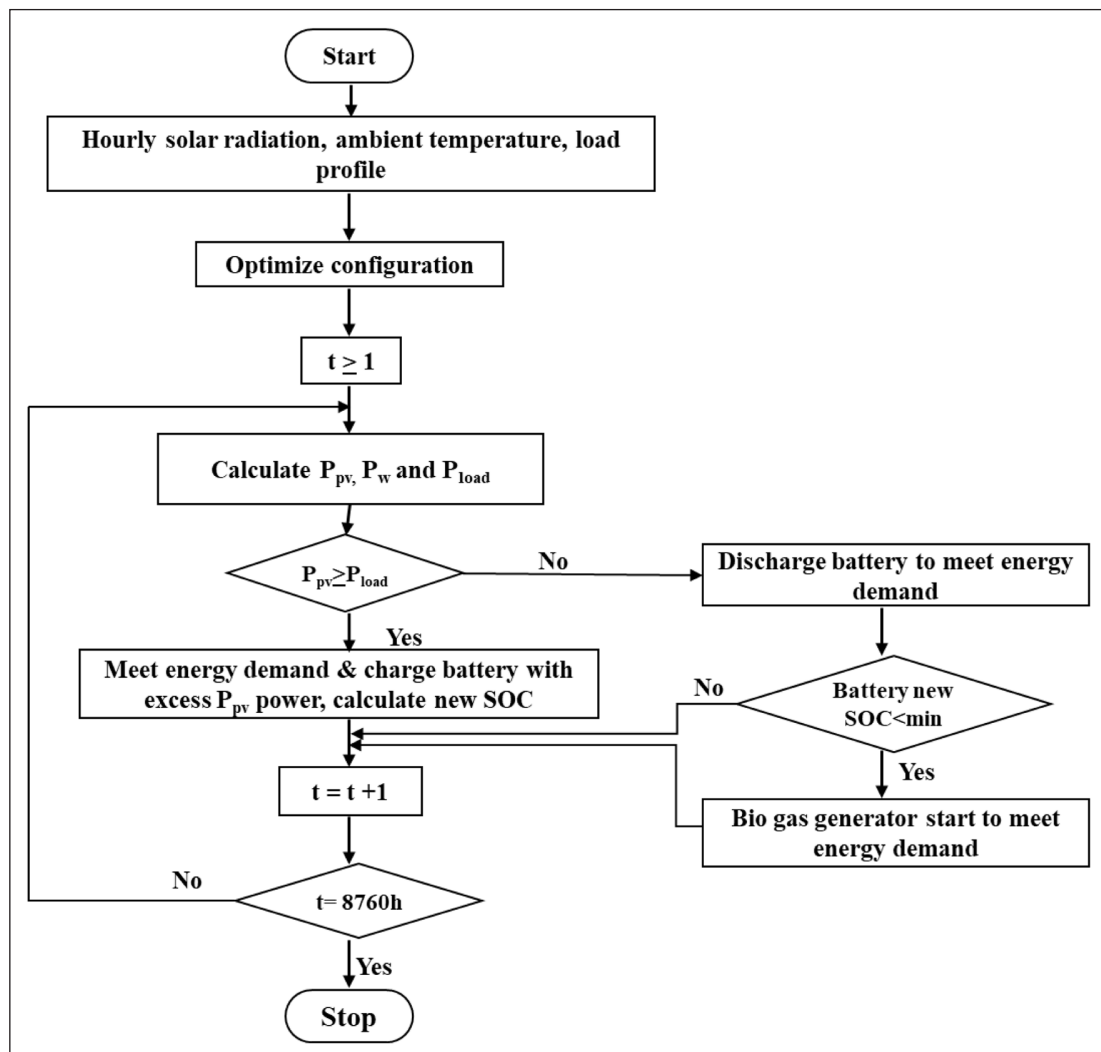


Figure 5: Flow chart of operational strategy of proposed HRES.

and viable operation. IRES systems involved in present study work in three modes (1) Wind turbine & Solar PV mode, (2) Battery bank mode, (3) Bio-generator mode. In proposed IRES wind turbine and solar PV are primary energy source because of zero fuel cost, low O&M, and zero emission. Whenever wind and PV energy is more than electric load demand excess energy is stored in the battery bank. When these energy sources are not sufficient to fulfill load demand, control algorithm checks if battery bank can fulfill the demand and if found above suitable SOC battery bank act as energy source. However, when battery bank is unable to supply the shortage biogas generator is used as last option with an aim to minimize emission of pollutants, operation, maintenance and fuel cost.

5. Results and discussion

In the present section based on optimization strategy results of the proposed hybrid system are discussed based on optimal size, economic and energy output of the system.

5.1. Optimal sizing analysis of integrated system components

The effectiveness of optimization strategy in the proposed system is demonstrated by finding the contribution of individual components involved namely wind turbine, PV, battery, biogas generator and converter system. Maximum wind, PV and battery usage is adopted to meet the electric load demand. The HOMER software simulates 2358 solutions based on technical and economic parameters to find the optimal configuration, out of which 783 were feasible and 1575 were not feasible due to capacity constraint. The optimisation process is based on net present cost. **Table 5** list some of the optimal feasible configurations of integrated hybrid renewable energy system. The combination are listed in descending order in terms of net present cost of the system. The most feasible configuration of IRES with minimum NPC and COE is combination of 12 kW solar Photovoltaics, 3 kW wind turbine, 15 kW biogas generator, 11 kW converter and energy storage back up with 40 battery (200 Ah, 12 V).

5.2. Economic analysis of hybrid system

The optimisation process is based on net present cost which is total capital cost, O&M cost, replacement cost and salvage cost of all components of integrated system over the project life. The NPC and COE of the optimum IRES are \$ 117,098 and \$ 0.09 per kWh respectively. **Table 6** lists net present cost breakdown analysis of optimum hybrid integrated energy system. It can be observed that the total cost of biogas system is maximum and account around 53% of total net present cost of the system followed by battery bank with 24%, solar PV with 13%, wind energy system with 5% and converter with 4%.

5.3. Energy analysis of hybrid system

The total energy generated by integrated hybrid energy system in complete year is 71,826 kWh to supply AC primary load of 64,396 kWh per year. The energy output of 12 kW

PV is 18,708 kWh/year with mean output of 51.3 kWh/day and has penetration factor of 29%. The energy output of wind turbine is 1,726 kWh/year and has penetration factor of 2.68%. The energy output of 15 kW biogas generator is 51,392 kWh/year with specific fuel consumption of 2.15 kg/kWh and mean electrical efficiency of 30.4%. The generator operate for 4,195 hours/year and has operational life of 4.85 years. The battery bank has autonomy of 3.27 hours with 11,486 kWh energy input, 9,198 kWh of energy output and 2,298 kWh of energy losses for a year. The expected life of battery is 4.11 years. The 11 kW inverter has capacity factor of 20.9% with 6,004 hours of operation in a year. The energy input, output and losses for inverter are 21,785 kWh, 20,695 kWh and 1,089 kWh for a year respectively. The 11 kW rectifier has capacity factor of 6.92% with 2,619 hours of operation in a year. The energy input, output and losses for rectifier are 7,204 kWh, 6,844 kWh and 360 kWh for a year respectively. The month wise percentage contribution of wind turbine, solar PV and biogas generator is shown in **Figure 6**.

The hourly usage pattern of individual components is also important to know each components' potential to satisfy load demand. **Figure 7** shows power output of wind energy system on hourly basis for the complete year. The power output of wind turbine is related with wind speed and have more output during the month with higher wind speed. **Figure 8** shows power output of PV system on hourly basis for the complete year. It can be observed that power generation is related to solar radiation intensity, during the sunny days power generation is more whereas there is decline during the rainy and winter days. Further, during the peak day time (11:00 am to 2:00 pm) the power generation by solar PV is more which is sufficient to meet load demand and excess power is stored in the battery bank. **Figure 9** shows operational performance of battery bank on hourly basis. The battery bank life depend upon its charge and discharge cycle level. During the time when battery SOC reach below threshold level the biogas generator come in operation to meet the load demand. **Figure 10** shows power output of biogas generator on hourly basis. The biogas generator operates for 2,304 hours in the complete year with 893 number of starts.

6. Sensitivity analysis of system

Sensitivity analysis is important as it helps us to predict the behavior of the system under different conditions. For the present hybrid renewable energy system sensitivity analysis has been done with variation of wind turbine cost, PV cost, battery cost, bio-gen cost.

6.1. Variation in wind turbine cost

The net present cost and cost of energy of the hybrid system has been evaluated by variation in wind turbine cost. The wind turbine cost has been varied from 0.8 to 1.3 times to its present capital cost. The NPC and CoE of the system varied from \$ 116,108 to \$ 118,608 and \$ 0.088/kWh to \$ 0.093/kWh respectively. The variation in NPC and CoE with change in wind turbine cost are shown in **Figure 11**.

Table 5: Different configuration of some of the viable combination of integrated hybrid energy systems.

Combination	Solar PV (kW)	Wind turbine (kW)	Bi-gen (kW)	Battery (no.)	Converter (kW)	COE (\$/kWh)	Total NPC (\$)	Operating cost (\$/yr)	Initial capital (\$)	Bio-gen (kWh/yr)	Solar PV (kWh/yr)	Wind turbine (kWh/yr)	Battery Autonomy (hr)	Battery Usable Nominal Cap (kWh)
1	12	3	15	40	11	0.090	117098.1	6621.1	31503.9	51391.8	18708.2	1726.4	3.27	24.02
2	13	3	15	40	12	0.091	117288.7	6558.3	32506.5	50153.4	20267.2	1726.4	3.27	24.02
3	14	3	15	39	11	0.091	117305.4	6506.7	33190.1	49335.5	21826.3	1726.4	3.19	23.42
4	13	3	15	40	12	0.091	117432.7	6561.6	32608.0	50086.3	20267.2	1726.4	3.27	24.02
5	14	3	15	39	12	0.091	117592.4	6510.5	33427.3	49146.5	21826.3	1726.4	3.19	23.42
6	16	3	15	39	12	0.092	117988.0	6404.1	35199.0	47195.0	24944.3	1726.4	3.19	23.42
7	16	3	15	40	12	0.092	118195.4	6409.0	35342.8	47128.8	24944.3	1726.4	3.27	24.02
8	13	3	15	40	14	0.092	118331.7	6600.7	33001.3	50086.3	20267.2	1726.4	3.27	24.02
9	15	3	15	40	16	0.094	119761.6	6534.6	35284.9	48018.6	23385.3	1726.4	3.27	24.02
10	14	6	15	39	12	0.097	122569.8	6520.0	38282.0	47624.8	21826.3	3452.8	3.19	23.42
11	14	6	15	40	12	0.097	122596.5	6510.6	38430.6	47454.6	21826.3	3452.8	3.27	24.02
12	11	6	15	40	13	0.097	122617.5	6711.4	35856.3	50830.5	17149.2	3452.8	3.27	24.02
13	15	6	15	39	12	0.098	122980.3	6472.0	39313.6	46567.6	23385.3	3452.8	3.19	23.42
14	16	6	15	39	12	0.098	123314.7	6426.3	40238.6	45647.5	24944.3	3452.8	3.19	23.42
15	11	9	15	40	11	0.103	126981.2	6685.5	40553.6	49254.8	17149.2	5179.2	3.27	24.02

Table 6: Net present cost breakdown analysis of optimum hybrid integrated energy system.

Component	Principal cost (in \$)	O & M cost (in \$)	Replacement cost (in \$)	Fuel cost (in \$)	Salvage cost (in \$)	Total (\$)
Wind turbine	5,000.00	1,939.13	0.00	0.00	0.00	6,939.13
Solar PV	11,100.00	3,878.25	0.00	0.00	0.00	14,478.25
Solar inverter and control panel	2,233.94	1,166.84	1,973.55	0.00	267.58	5,106.76
Battery	6,120.00	3,619.70	19,495.61	0.00	1,156.56	28,078.75
Biogas-generator	7,050.00	10,073.77	16,973.19	28,589.51	691.27	61,995.19
Complete IRES	31,503.94	20,677.70	38,442.35	28,589.51	2,115.41	117,098.09

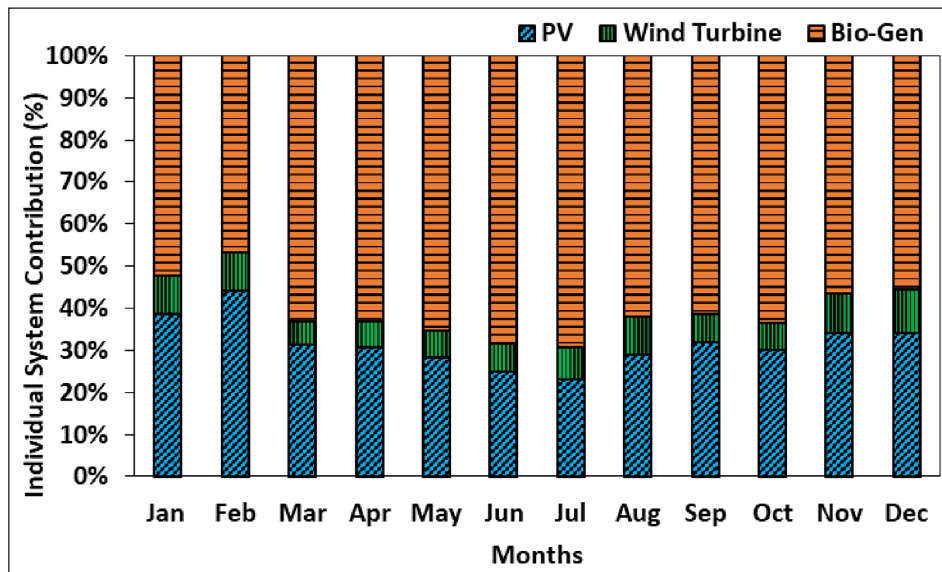


Figure 6: Monthly contribution of individual system components.

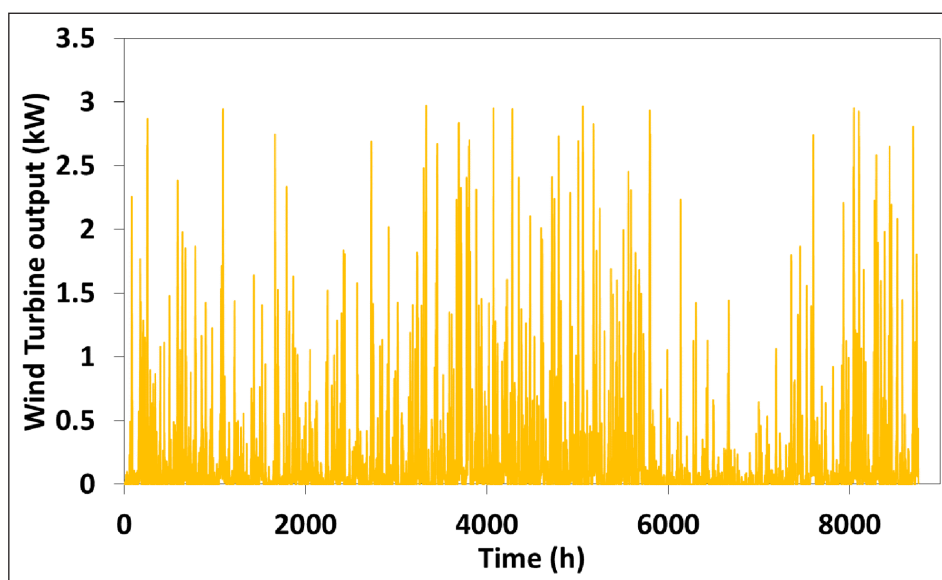


Figure 7: Yearly Wind turbine output performance.

6.2. Variation in PV cost

The net present cost and cost of energy of the hybrid system has been evaluated by variation in solar photovoltaic cost. The PV cost has been varied from 0.8 to 1.3 times to

its present capital cost. The NPC and CoE of the system varied from \$ 114,888 to \$ 120,438 and \$ 0.086/kWh to \$ 0.097/kWh/h respectively. The variation in NPC and CoE for change in PV cost are shown in **Figure 12**.

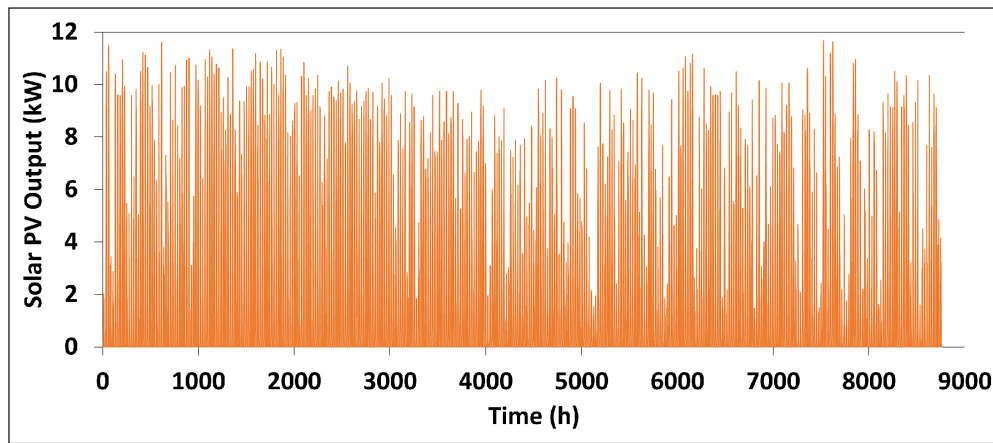


Figure 8: Yearly PV output performance.

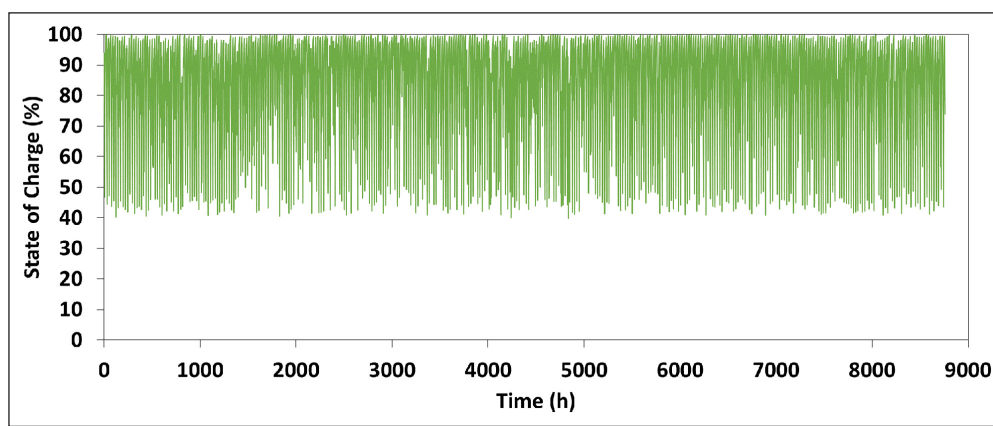


Figure 9: Yearly battery bank performance.

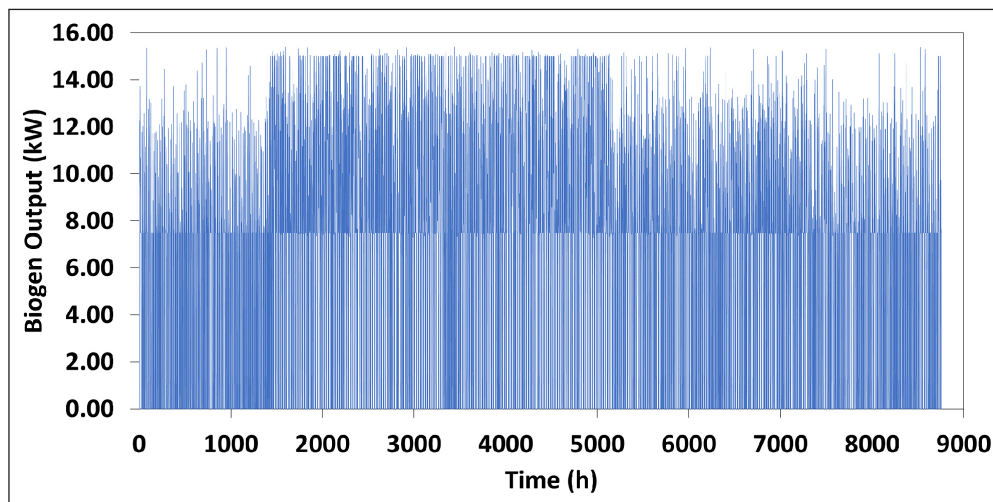


Figure 10: Yearly Bio-Gen output performance.

6.3. Variation in battery cost

The net present cost and cost of energy of the hybrid system has been evaluated by variation in battery cost. The battery cost has been varied from 0.8 to 1.3 times to its present capital cost. The NPC and CoE of the system varied from \$ 115,884 to \$ 118,944 and \$ 0.88/kWh to \$ 0.93/kWh respectively. The variation in NPC and CoE for change in battery cost are shown in **Figure 13**.

6.4. Variation in bio-gen cost

The net present cost and cost of energy of the hybrid system has been evaluated by variation in bio generator cost. The generator cost has been varied from 0.8 to 1.3 times to its present capital cost. The NPC and CoE of the system varied from \$ 115,698 to \$ 119,223 and \$ 0.88/kWh to \$ 0.93/kWh respectively. The variation in NPC and CoE for change in battery cost are shown in **Figure 14**.

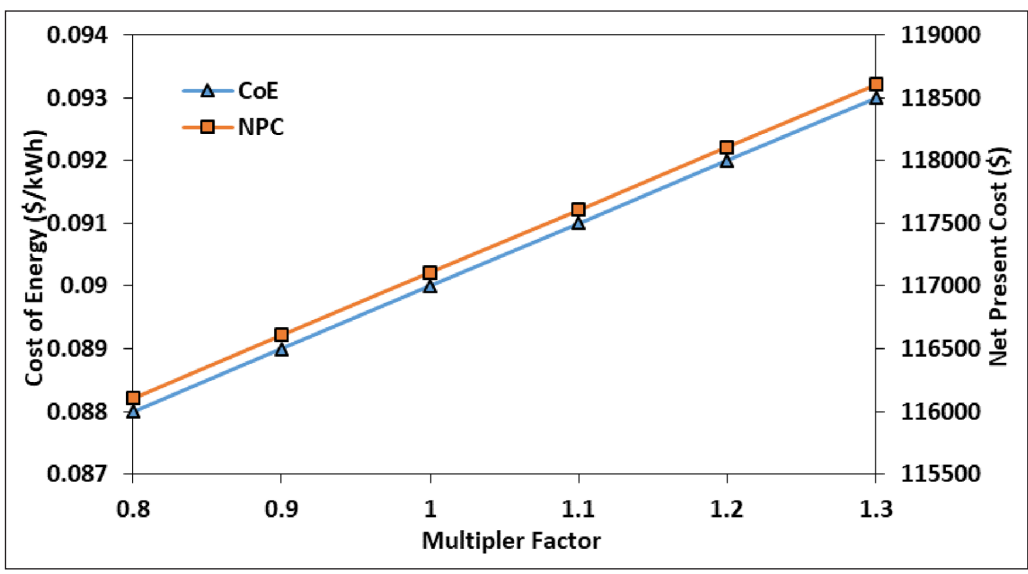


Figure 11: CoE and NPC analysis of hybrid system with variation in wind turbine cost.

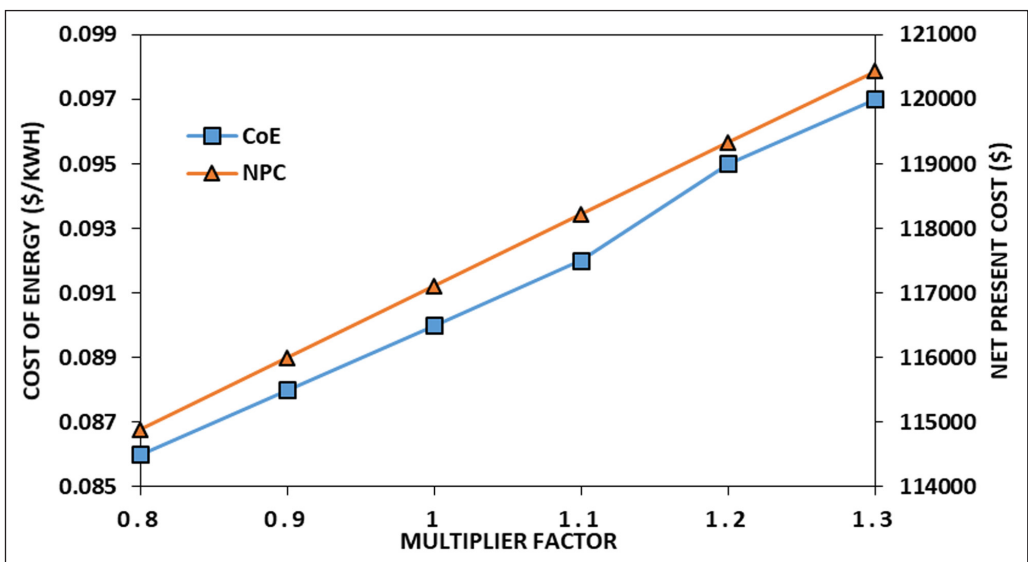


Figure 12: CoE and NPC analysis of hybrid system with variation in PV cost.

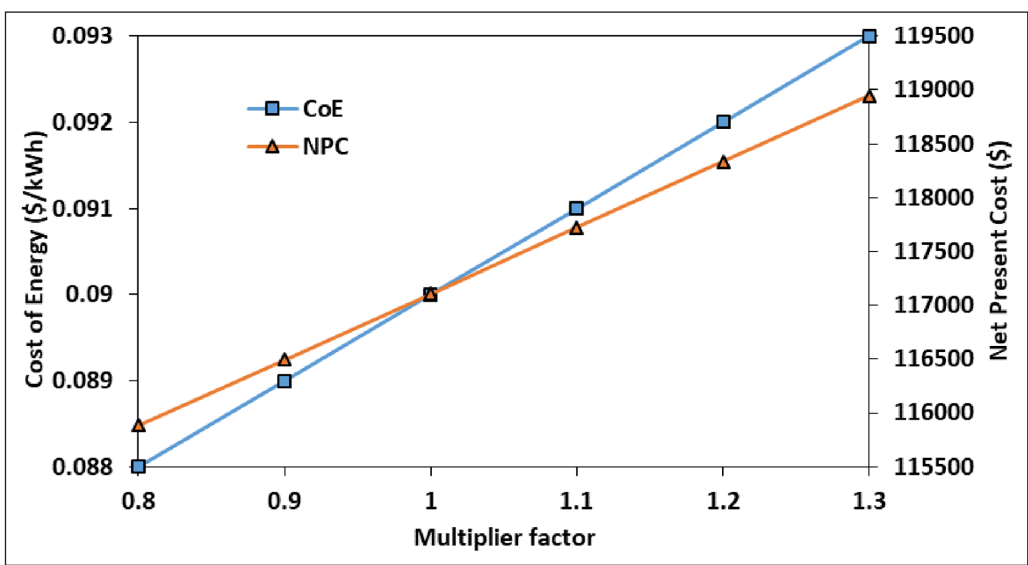


Figure 13: CoE and NPC analysis of hybrid system with variation in battery cost.

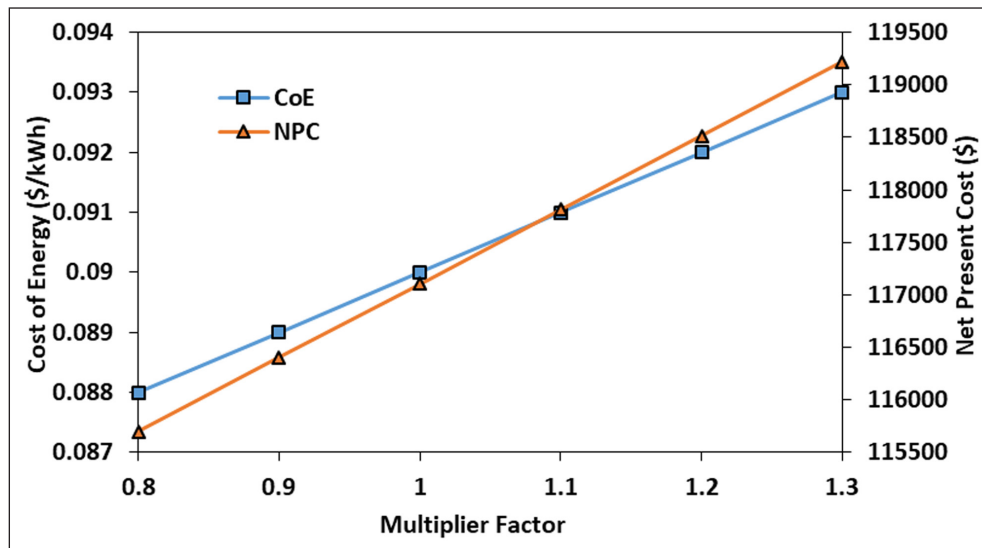


Figure 14: CoE and NPC analysis of hybrid system with variation in bio-gen cost.

7. Conclusion

In the present study, a hybrid integrated energy system has been investigated using wind turbine, solar PV, and biogas generator as different source component to meet electric load demand. The design, modeling and operation of each system component had been described in detail. The optimization of the integrated system has been optimized by varying the size of the individual components as well as operational strategy. HOMER tool was used to optimize the overall system so as to have maximum renewable energy contribution with minimum net present cost. The most feasible system consists of 12 kW Photovoltaics, 3 kW wind turbine and 15 kW biogas generator with net present cost and cost of energy equal to \$ 117,098.1 and \$ 0.090/kWh unit respectively. Also, sensitivity analysis of hybrid renewable system has been done with variation in solar PV, wind turbine, battery and biogas generator cost. The IRES generates 71,826 kWh to meet AC load of 64,396 kWh per year. The capacity factor and percentage contribution of PV, wind turbine and biogas generator are 17.8%, 6.57%, 39.1% and 26%, 2.4%, 71.6% respectively. The results show that integrated system is very sensitive with variation in prices of components.

Nomenclature

A_w	Wind turbine swept area (m ²)
C_{bat}	Capacity of battery
C_{VBG}	Calorific value of biogas (MJ/kg)
C_{NPC}	Net present cost
C_{ann}	Annualized cost
C_{rep}	Component's replacement cost
E_{pv}	Electrical output of PV system (W)
E_{load}	Energy demand (kWh)
f	Expected inflation rate
I_{sc}	Short circuit current of PV module (A)
I_{bat}	Battery current (A)
I_T	Solar irradiance at tilted PV (W/m ²)
I	Annual real discount rate
i'	Nominal discount rate
N_s	PV modules connected in parallel

N_p	PV modules connected in series
P_w	Power output of Wind turbine (kW)
P_{Weff}	Effective electrical power output of wind turbine (kW)
P_{pv}	Power output of solar PV array (W)
P_{ar}	Effective power output from PV array (W)
P_{bio}	Power generation by biogas generator (W)
P_{load}	Power load demand (W)
R_{proj}	Project lifetime
R_{rem}	Component's remaining life
R_{comp}	Lifetime of the project
S_{stc}	Incident solar radiation at standard test condition (W/m ²)
S_{mod}	Solar radiation incident on the module (W/m ²)
S_{inc}	Solar radiation perpendicular to the sun (W/m ²)
$T_{PV,avg}$	Average Temperature of PV (°C)
T_{amb}	Ambient temperature (°C)
t	Duration of operation
V_{oc}	Open circuit voltage of PV module (V)
$V_{ci'}$	Wind turbine cut in speed (m/s)
V_r	Wind turbine rated speed (m/s)
V_{co}	Wind turbine cut out speed (m/s)
V_{bat}	Terminal voltage of battery (V)

Abbreviations

AD	Daily autonomy
CRC	Classroom complex
CRF	Capital recovery factor
DOD	Depth of discharge of battery
FF	Fill factor of PV panel
HOMER	Hybrid optimization of multiple energy resources
IRES	Integrated renewable energy system
NOCT	Nominal operating cell temperature (°C)
PV	Photovoltaics
SOC	State of charge of the battery

Greek symbol

β_c	PV panel temperature coefficient
γ_c	Solar irradiance coefficient
δ	Latitude degrees

σ	Battery self-discharge rate
η_{bat}	Battery charge efficiency
η_{bat}	Battery efficiency
η_{BG}	Efficiency of biogas generator
η_{gas}	Efficiency of gasification of gasifier
η_{w}	Efficiency of wind turbine
η_{inv}	Efficiency of inverter
η_{mod}	PV module efficiency
η_{stc}	Efficiency of PV module at standard test condition

Competing Interests

The authors have no competing interests to declare.

References

- Al-falahi, MDA, Jayasinghe, SDG and Enshaei, H.** 2017. A review on recent size optimization methodologies for standalone solar and wind hybrid renewable energy system. *Energy Convers. Manag.*, 143: 252–274. DOI: <https://doi.org/10.1016/j.enconman.2017.04.019>
- Al Garni, HZ, Awasthi, A and Ramli, MAM.** 2018. Optimal design and analysis of grid-connected photovoltaic under different tracking systems using HOMER. *Energy Convers. Manag.*, 155: 42–57. DOI: <https://doi.org/10.1016/j.enconman.2017.10.090>
- Allison, J.** 2017. Robust multi-objective control of hybrid renewable microgeneration systems with energy storage. *Appl. Therm. Eng.*, 114: 1498–1506. DOI: <https://doi.org/10.1016/j.applthermaleng.2016.09.070>
- Baghdadi, F, Mohammedi, K, Diaf, S and Behar, O.** 2015. Feasibility study and energy conversion analysis of stand-alone hybrid renewable energy system. *Energy Convers. Manag.*, 105: 471–479. DOI: <https://doi.org/10.1016/j.enconman.2015.07.051>
- Behzadi Forough, A and Roshandel, R.** 2017. Multi objective receding horizon optimization for optimal scheduling of hybrid renewable energy system. *Energy Build*, 150: 583–597. DOI: <https://doi.org/10.1016/j.enbuild.2017.06.031>
- Borges Neto, MR, Carvalho, PCM, Carioca, JOB and Canafistula, FJF.** 2010. Biogas/photovoltaic hybrid power system for decentralized energy supply of rural areas. *Energy Policy*, 38: 4497–4506. DOI: <https://doi.org/10.1016/j.enpol.2010.04.004>
- Bosch Solar Energy.** n.d. Properties of Bosch Solar Module c-Si M 60. *Bosch Solar Energy Corporation*.
- Cano, MH, Agbossou, K, Kelouwani, S and Dube, Y.** 2017. Experimental evaluation of a power management system for a hybrid renewable energy system with hydrogen production. *Renew. Energy*, 113: 1086–1098. DOI: <https://doi.org/10.1016/j.renene.2017.06.066>
- Castellanos, JG, Walker, M, Poggio, D, Pourkashanian, M and Nimmo, W.** 2015. Modelling an off-grid integrated renewable energy system for rural electrification in India using photovoltaics and anaerobic digestion. *Renew. Energy*, 74: 390–398. DOI: <https://doi.org/10.1016/j.renene.2014.08.055>
- Chauhan, A and Saini, RP.** 2014. A review on integrated renewable energy system based power generation for stand-alone applications: configurations, storage options, sizing methodologies and control. *Renew. Sustain. Energy Rev.*, 38: 99–120. DOI: <https://doi.org/10.1016/j.rser.2014.05.079>
- Chauhan, A and Saini, RP.** 2016. Techno-economic optimization based approach for energy management of a stand-alone integrated renewable energy system for remote areas of India. *Energy*, 94: 138–156. DOI: <https://doi.org/10.1016/j.energy.2015.10.136>
- Chedid, R, Akiki, H and Rahman, S.** 1998. A decision support technique for the design of hybrid solar-wind power systems. *IEEE Trans. Energy Convers.*, 13: 76–83. DOI: <https://doi.org/10.1109/60.658207>
- Chiasson, J and Vairamohan, B.** 2005. Estimating the State of Charge of a Battery. *IEEE Trans. Control Syst. Technol.*, 13: 465–470. DOI: <https://doi.org/10.1109/TCST.2004.839571>
- Chong, LW, Wong, YW, Rajkumar, RK, Rajkumar, RK and Isa, D.** 2016. Hybrid energy storage systems and control strategies for stand-alone renewable energy power systems. *Renew. Sustain. Energy Rev.*, 66: 174–189. DOI: <https://doi.org/10.1016/j.rser.2016.07.059>
- Dalton, GJ, Lockington, DA and Baldock, TE.** 2008. Feasibility analysis of stand-alone renewable energy supply options for a large hotel. *Renew. Energy*, 33: 1475–1490. DOI: <https://doi.org/10.1016/j.renene.2007.09.014>
- Derrouazin, A, Aillerie, M, Mekkakia-Maaza, N and Charles, JP.** 2017. Multi input-output fuzzy logic smart controller for a residential hybrid solar-wind-storage energy system. *Energy Convers. Manag.*, 148: 238–250. DOI: <https://doi.org/10.1016/j.enconman.2017.05.046>
- Giatrakos, GP, Tsoutsos, TD, Mouchtaropoulos, PG, Naxakis, GD and Stavrakakis, G.** 2009. Sustainable energy planning based on a stand-alone hybrid renewable energy/hydrogen power system: Application in Karpathos island, Greece. *Renew. Energy*, 34: 2562–2570. DOI: <https://doi.org/10.1016/j.renene.2009.05.019>
- Goel, S and Sharma, R.** 2017. Performance evaluation of stand alone, grid connected and hybrid renewable energy systems for rural application: A comparative review. *Renew. Sustain. Energy Rev.*, 78: 1378–1389. DOI: <https://doi.org/10.1016/j.rser.2017.05.200>
- Indian Meteorological Department [WWW Document].** n.d. URL <http://www.imd.gov.in/Welcome%20To%20IMD/Welcome.php>.
- Kabalci, E.** 2013. Design and analysis of a hybrid renewable energy plant with solar and wind power. *Energy Convers. Manag.*, 72: 51–59. DOI: <https://doi.org/10.1016/j.enconman.2012.08.027>
- Khanna, S, Reddy, KS and Mallick, TK.** 2017. Performance analysis of tilted photovoltaic system integrated with phase change material under varying operating conditions. *Energy*, 133: 887–899. DOI: <https://doi.org/10.1016/j.energy.2017.05.150>

- Khanna, S, Reddy, KS and Mallick, TK.** 2018. Effect of climate on electrical performance of finned phase change material integrated solar photovoltaic. *Sol. Energy*, 174: 593–605. DOI: <https://doi.org/10.1016/j.solener.2018.09.023>
- Koutroulis, E, Kolokotsa, D, Potirakis, A and Kalaitzakis, K.** 2006. Methodology for optimal sizing of stand-alone photovoltaic/wind-generator systems using genetic algorithms. *Sol. Energy*, 80: 1072–1088. DOI: <https://doi.org/10.1016/j.solener.2005.11.002>
- Lau, KY, Yousof, MFM, Arshad, SNM, Anwari, M and Yatim, AHM.** 2010. Performance analysis of hybrid photovoltaic/diesel energy system under Malaysian conditions. *Energy*, 35: 3245–3255. DOI: <https://doi.org/10.1016/j.energy.2010.04.008>
- Li, C, Ge, X, Zheng, Y, Xu, C, Ren, Y, Song, C and Yang, C.** 2013. Techno-economic feasibility study of autonomous hybrid wind/PV/battery power system for a household in Urumqi, China. *Energy*, 55: 263–272. DOI: <https://doi.org/10.1016/j.energy.2013.03.084>
- Liu, G, Li, M, Zhou, B, Chen, Y and Liao, S.** 2018. General indicator for techno-economic assessment of renewable energy resources. *Energy Convers. Manag.*, 156: 416–426. DOI: <https://doi.org/10.1016/j.enconman.2017.11.054>
- Munuswamy, S, Nakamura, K and Katta, A.** 2011. Comparing the cost of electricity sourced from a fuel cell-based renewable energy system and the national grid to electrify a rural health centre in India: A case study. *Renew. Energy*, 36: 2978–2983. DOI: <https://doi.org/10.1016/j.renene.2011.03.041>
- Muselli, M, Notton, G and Louche, A.** 1999. Design of hybrid-Photovoltaic power generator, with optimization of energy management. *Sol. Energy*, 65: 143–157. DOI: [https://doi.org/10.1016/S0038-092X\(98\)00139-X](https://doi.org/10.1016/S0038-092X(98)00139-X)
- Ozden, E and Tari, I.** 2016. Energy-exergy and economic analyses of a hybrid solar-hydrogen renewable energy system in Ankara, Turkey. *Appl. Therm. Eng.*, 99: 169–178. DOI: <https://doi.org/10.1016/j.applthermaleng.2016.01.042>
- Patil, ABK, Saini, RP and Sharma, MP.** 2010. Integrated renewable energy systems for off grid rural electrification of remote area. *Renew. Energy*, 35: 1342–1349. DOI: <https://doi.org/10.1016/j.renene.2009.10.005>
- Perez-Navarro, A, Alfonso, D, Ariza, HE, Carcel, J, Correcher, A, Escriva-Escriva, G, Hurtado, E, Ibanez, F, Penalvo, E, Roig, R, Roldan, C, Sanchez, C, Segura, I and Vargas, C.** 2016. Experimental verification of hybrid renewable systems as feasible energy sources. *Renew. Energy*, 86: 384–391. DOI: <https://doi.org/10.1016/j.renene.2015.08.030>
- Rahman, MM, Hasan, MM, Paatero, JV and Lahdelma, R.** 2014. Hybrid application of biogas and solar resources to fulfill household energy needs: A potentially viable option in rural areas of developing countries. *Renew. Energy*, 68: 35–45. DOI: <https://doi.org/10.1016/j.renene.2014.01.030>
- Reddy, KS, Mudgal, V and Mallick, TK.** 2017. Thermal performance analysis of multi-phase change material layer-integrated building roofs for energy efficiency in built-environment. *Energies*, 10. DOI: <https://doi.org/10.3390/en10091367>
- Reddy, KS, Mudgal, V and Mallick, TK.** 2018. Review of latent heat thermal energy storage for improved material stability and effective load management. *J. Energy Storage*, 15: 205–227. DOI: <https://doi.org/10.1016/j.est.2017.11.005>
- Shi, Z, Wang, R and Zhang, T.** 2015. Multi-objective optimal design of hybrid renewable energy systems using preference-inspired coevolutionary approach. *Sol. Energy*, 118: 96–106. DOI: <https://doi.org/10.1016/j.solener.2015.03.052>
- Singh, A, Baredar, P and Gupta, B.** 2017. Techno-economic feasibility analysis of hydrogen fuel cell and solar photovoltaic hybrid renewable energy system for academic research building. *Energy Convers. Manag.*, 145: 398–414. DOI: <https://doi.org/10.1016/j.enconman.2017.05.014>
- Specification, Test generator. Sawafuji Electric Co., Ltd, ELEMEX Generator SH7600EX: Owner's Manual, n.d.
- Sukhatme, K and Sukhatme, SP.** 1996. Solar energy: principles of thermal collection and storage, 2nd ed. Tata McGrawHill.
- Taele, BM, Mokhutsoane, L, Hapazari, I, Tlali, SB and Senatla, M.** 2012. Grid electrification challenges, photovoltaic electrification progress and energy sustainability in Lesotho. *Renew. Sustain. Energy Rev.*, 16: 973–980. DOI: <https://doi.org/10.1016/j.rser.2011.09.019>
- Tezer, T, Yaman, R and Yaman, G.** 2017. Evaluation of approaches used for optimization of stand-alone hybrid renewable energy systems. *Renew. Sustain. Energy Rev.*, 73, 840–853. DOI: <https://doi.org/10.1016/j.rser.2017.01.118>
- Tito, SR, Lie, TT and Anderson, TN.** 2016. Optimal sizing of a wind-photovoltaic-battery hybrid renewable energy system considering socio-demographic factors. *Sol. Energy*, 136: 525–532. DOI: <https://doi.org/10.1016/j.solener.2016.07.036>
- Yilmaz, S and Selim, H.** 2013. A review on the methods for biomass to energy conversion systems design. *Renew. Sustain. Energy Rev.*, 25: 420–430. DOI: <https://doi.org/10.1016/j.rser.2013.05.015>
- Yin, C, Wu, H, Locment, F and Sechilariu, M.** 2017. Energy management of DC microgrid based on photovoltaic combined with diesel generator and supercapacitor. *Energy Convers. Manag.*, 132: 14–27. DOI: <https://doi.org/10.1016/j.enconman.2016.11.018>
- Zahboune, H, Zouggar, S, Krajacic, G, Varbanov, PS, Elhafyani, M and Ziani, E.** 2016. Optimal hybrid renewable energy design in autonomous system using modified electric system cascade analysis and Homer software. *Energy Convers. Manag.*, 126: 909–922. DOI: <https://doi.org/10.1016/j.enconman.2016.08.061>

How to cite this article: Mudgal, V, Reddy, KS and Mallick, TK. 2019. Techno-Economic Analysis of Standalone Solar Photovoltaic-Wind-Biogas Hybrid Renewable Energy System for Community Energy Requirement. *Future Cities and Environment*, 5(1): 11, 1–16. DOI: <https://doi.org/10.5334/fce.72>

Submitted: 28 May 2019

Accepted: 09 October 2019

Published: 07 November 2019

Copyright: © 2019 The Author(s). This is an open-access article distributed under the terms of the Creative Commons Attribution 4.0 International License (CC-BY 4.0), which permits unrestricted use, distribution, and reproduction in any medium, provided the original author and source are credited. See <http://creativecommons.org/licenses/by/4.0/>.

]u[

Future Cities and Environment, is a peer-reviewed open access journal published by Ubiquity Press.

OPEN ACCESS 